J. Fluid Mech. (1990), vol. 219, pp. 119–142
Printed in Great Britain

On accurately measuring statistics associated with small-scale structure in turbulent boundary layers using hot-wire probes

By J. C. KLEWICKI AND R. E. FALCO
Turbulence Structure Laboratory, Department of Mechanical Engineering,
Michigan State University, East Lansing, MI 48824-1226, USA

(Received 12 September 1989)

Spanwise vorticity measurements have been performed in zero-pressure-gradient boundary layers over the range $1010 < R_\theta < 4850$ ($R_\theta \equiv U_\infty \theta/\nu$, where U_∞ is the free-stream velocity and θ is the momentum deficit thickness) using a four-wire probe. In addition, experiments quantifying the spatial and temporal resolution required to obtain an accurate statistical representation of the small-scale structure of wall-bounded turbulence were performed. Furthermore, a thorough investigation of statistical convergence for a variety of fluctuating quantities was performed. Comparisons with earlier high-resolution studies indicate that the maximum value of u'/u_τ increases with increasing Reynolds number over the given R_θ range ($u' \equiv$ r.m.s. u, and u_τ is the friction velocity). It is suggested that detecting this dependence provides a good measure of probe resolution. In general it was found that statistics of velocity gradients were distinctly more sensitive to finite probe size than velocity statistics. Wire spacing experiments suggest that Wyngaard's (1969) criterion is to a good approximation valid even under anisotropic conditions. Furthermore, it was found that instantaneously spatial averaging of $\partial u/\partial t$ caused significant attenuation in the resulting r.m.s., and that this averaging procedure is sensitive to the level of mean shear. A simple method of estimating how noise in the u-velocity signals enters into the $\partial u/\partial y$ signals is presented. The convergence study shows that statistical convergence criteria developed from free-shear flows severely underestimates the averaging times required in boundary layers. A table of general convergence criteria is provided.

1. Introduction

Over the past thirty years studies of wall-bounded turbulent shear flows have identified the existence of coherent motions. To further understand the nature of these motions there has been an increased emphasis on the measurement of velocity-gradient quantities and their associated statistical properties. This increased emphasis stems from the general belief that coherent motions embody organized vorticity, or that they result from interactions involving organized vorticity.

As a rule of thumb, it is generally acknowledged that to resolve the smallest scales of motion in a turbulent flow the probe must be capable of resolving motions of approximately the Kolmogoroff scale, $\eta\,(\equiv(\nu^3/\epsilon)^{\frac{1}{4}})$. In the near-wall region of a fully turbulent boundary layer, say $y^+ \leqslant 50$, this corresponds to less than $5\nu/u_\tau$. Few flow facilities allow for studies that have the capability to achieve this resolution. Since multi-wire probes are needed to obtain time-resolved spatial gradients, both the

length of the hot wires and the spacing between them should, in principle, satisfy this criterion. The following partial survey gives an indication of resolutions and integration times that have been used in studies of wall-bounded turbulent shear flows measuring time-resolved velocity gradients and/or vorticity components.

Early boundary-layer studies used probes that were relatively large compared to the Kolmogorov scale. Corrsin & Kistler (1954) studied the intermittent region of a rough-wall turbulent boundary layer at $R_\theta \approx 7900$ using a streamwise vorticity probe designed by Kovasznay (1950). This probe's wire length, $l^+ \equiv lu_\tau/\nu$, was approximately 100 wall units, and the average wire spacing was ≈ 70 wall units. Kovasznay, Komoda & Vasudeva (1962) used a parallel array with spacing $y^+ \approx 8$, with wires of length $l^+ \approx 24$ to study the later stages of the transition process. The wire spacing in this study was about one-tenth of the boundary-layer thickness. Kovasznay, Kibens & Blackwelder (1970) used a pair of single-wire probes to detect the vorticity fronts and backs of the large-scale motions in a fully turbulent boundary layer at $R_\theta \approx 3100$. Their wires had a length of 25 wall units and a spacing that varied from 40 to 60 wall units (or about 10–16 Kolmogorov scales). Using the result of Wyngaard (1969), Blackwelder & Kovasznay (1970) estimate that this spacing resulted in resolving about 70% of the true r.m.s. $\partial u/\partial y$ gradient.

Later works involved more complicated multi-wire probes. These probes enabled one or more vorticity components to be measured. Eckelmann *et al.* (1977) studied ω_z and ω_y as close as $y^+ = 15$ in a channel flow at $R_{d/2} = 4000$ ($R_{d/2}$ is based upon the channel centreline velocity and half width). Their five-film probe had films with an average spacing and length of 1.75 wall units. An interesting additional point is that they found that non-dimensional averaging times, $2TU_c/d$, of greater than 5000 were needed to obtain stable ensemble averages. Falco (1980) using the same type of probe as in the present study, measured ω_z in a fully turbulent boundary layer at $y^+ = 16$ for $R_\theta = 1068$. The spatial scale of this probe was $l^+ = \Delta y^+ = 3.6$ and $\Delta z^+ = 11.5$. In this combined visualization/hot-wire study, approximately 210 boundary-layer thicknesses were observed. Kastrinakis (1977) in a study of turbulent channel flow using Kovasznay (1950)-type ω_x probes (with the average wire spacing, $h^+ \approx l^+ \approx 5$ at $R_{d/2} \approx 6250$) made both single and two-point ω_x measurements as close as $y^+ \approx 9$. However, further study of this probe by Kastriniakis, Eckelmann & Willmarth (1979) indicated that since the four wires were not independently operated the probe output was significantly sensitive to all three velocity components. Later Kastrinakis & Eckelmann (1983) measured streamwise vorticity with a four-wire (independently operated) probe in a fully developed channel flow as close as $y^+ \approx 19$ for $R_{d/2} = 12000$. This probe had $h^+ \approx 11.5, l^+ = 9.1$, and their record length was $2TU_c/d = 2670$. Subramanian, Kandola & Bradshaw (1985) studied the low-wavenumber aspects of ω_z in the outer part of a fully developed turbulent boundary layer at $R_\theta = 14500$. Their wire spacing for $\partial u/\partial y$ was ≈ 375 wall units, and their wire length was ≈ 75 wall units. Their averaging time was $TU_\infty/\delta \approx 7700$. Balint, Vukoslavčević & Wallace (1987*a*) in a study of a fully turbulent boundary layer at $R_\theta = 2100$ measured for the first time all three components of vorticity from $y^+ = 14.5$ to $y/\delta = 0.95$. This nine-wire probe had $h^+ = 8.9$ (J. M. Wallace, private communication), with wire lengths of $l^+ = 2.3$. Their averaging time was $TU_\infty/\delta \approx 3100$. More recently (Balint *et al.* 1987*b*) they have used a probe with an improved signal-to-noise ratio that had $h^+ = 10.4$ and $l^+ = 2.3$ at $R_\theta = 2850$. Klewicki (1989) using the apparatus described herein, has measured spanwise vorticity distributions and two-point ω_z correlations across turbulent boundary layers in the range $1010 \leqslant R_\theta \leqslant 4850$.

Using an array of two wires in a 'v' configuration that is embedded in the wall, it

is possible to obtain vorticity measurements in the immediate vicinity of the wall. Hogenes & Hanratty (1982) in a conditional-averaging study of turbulent pipe flow at $R_{d/2} = 18040$ used electrochemical probes with $l^+ \approx 8.5$, $\Delta z^+ \approx 3.8$, and $2TU_c/d = 540$. Blackwelder & Eckelmann (1979) studied the vorticity signatures at the wall associated with the bursting phenomena in a turbulent channel flow at $R_{d/2} = 3850$. The elements of their v-array were positioned at 45° to the mean flow direction. Their films' length were $l^+ = 1.3$, and were spaced $\Delta z^+ = 5.3$ apart. The averaging time used was $2TU_c/d = 3440$. Kreplin & Eckelmann (1979), also using the Gottingen oil channel, used v-array probes to obtain long-time-averaged statistics. Using the same probe at the same Reynolds number as Blackwelder & Eckelmann, they determined that an averaging time of $2TU_c/d = 2870$ was required to obtain 'adequate' convergence of velocity statistics up to the fourth moment.

Recently Alfredsson *et al.* (1988) have attempted to clarify sources of measurement error using wall-shear-stress sensors, and hot-wire/film probes in the sublayer. With respect to probe resolution effects, they found that for streamwise velocity measurements in the sublayer, probes of length $l^+ = 2$ and 10 resulted in no differences within experimental error. (Measurements made with a probe of $l^+ = 8$ in air resulted in discrepancies that were attributed to wall heat transfer effects). The range of their experiments included Reynolds numbers up to approximately $R_\theta = 2800$.

The above partial survey gives an indication of the resolution of experimental studies. Pertinent to understanding flow physics, questions then arise concerning what resolution is necessary to resolve the origin of coherent events. Early visual studies (for example Kline *et al.* 1967) have shown that important motions of the order of the sublayer thickness exist in the near-wall region. Probe studies support these results. Emmerling (1973) using an array of interferometric wall pressure transducers (of scale ≈ 54 viscous units) in a turbulent boundary layer at $R_\theta = 2000$ found examples of strong pressure disturbances that were about $\frac{1}{10}$ the transducer size. Schewe (1979) (working in the same tunnel at $R_\theta \approx 1400$) showed that trends in the wall pressure intensity, skewness, kurtosis and the frequency of occurrence of pressure peaks continue to change with decreasing transducer size. Even for his smallest diameter transducer, $d^+ = 19$, there was no indication that these trends had levelled-off. Willmarth & Bogar (1977) (working in a boundary layer at $R_\theta = 11700$ with $\times$-arrays having $l^+ = s^+ = 2.5$; s being the spacing between a pair of $\times$-wires) estimated that velocity gradients 'in the small scale structure near the wall will only become small over a distance that is less than approximately $\frac{1}{20}$ of the Kolmogoroff length'. Later Willmarth & Sharma (1984) using probes of length less than $1.0\nu/u_\tau$ (at $R_\theta = 6840$ and 9840) give direct evidence for the existence of near-wall 'shear layer fluctuations whose scale is of the order of the viscous length'. On the other hand, Johnson & Eckelmann (1983) working in the Gottingen oil channel at $R_{d/2} = 3800$ and using x-films with $l^+ \approx s^+ \simeq 1.7$ did not find evidence of this ultra-small-scale structure. However, as they noted, their Reynolds number was approximately thirty times lower than that of Willmarth & Bogar.

To date, reliable experimental guidelines related to obtaining an accurate statistical representation of wall turbulence are incomplete. Numerous problems have hindered progress in quantifying the turbulent motions that form and interact near the wall, but perhaps the most prevalent of these concerns the spatial resolution of the measurement probes. Uberoi & Kovasznay (1953) were the first to show analytically that for isotropic turbulence the output of a hot wire is attenuated as the length of the wire is increased. In an experimental study of the spatial resolution of

single-wire probes, Johansson & Alfredsson (1983) found significant attenuation in the measured value of u' due to spatial averaging caused by finite wire length. They also concluded that Reynolds-number effects are small compared with spatial averaging effects. Similar results have been found in boundary layers by Willmarth & Sharma (1984) and Ligrani & Bradshaw (1987). Ligrani & Bradshaw concluded that for studies outside of the sublayer adequate resolution for single-wire probes may be obtained if $l^+ \leqslant 20$, and the wire length-to-diameter ratio is $l/d > 200$. Furthermore, they showed that at $y^+ = 17$ significant changes in the high-frequency end of the u-velocity component spectrum occur for variations in l^+ from 14.0 to 3.3. Mestayer (1982), using Wyngaard's (1968) correction, showed that significant attenuation occurs in the high-wavenumber spectra of u and especially v for s/η and l/η both equal to 4.5. Since vorticity is concentrated in the higher wavenumbers, the equally accurate measurement of derivative quantities probably requires even better resolution. Furthermore, the accuracy of derivative measurements as obtained by two wires is degraded by problems additional to finite wire length. Antonia, Browne & Chambers (1985) indicate that the most important of these are the unequal time constants of the wires, mismatch in the wire calibrations, and the effects of finite wire separation.

Most analytical studies of the effect of finite wire spacing in multi-wire arrays, such as Wyngaard (1968, 1969), and Roberts (1973), use isotropic assumptions. A recent compilation by Browne, Antonia & Shah (1987) shows that many turbulent shear flows (and especially wall-bounded flows) exhibit significant levels of anisotropy. Thus, the validity of the results of the above analytical studies under anisotropic conditions is uncertain. As probes of smaller non-dimensional scale are used, presumably a more accurate representation of a probability distribution can be obtained. It is unclear, however, how the additional fine-scale information obtained through enhanced resolution of wall-region motions affects the convergence of statistics.

The purpose of the present study is to examine some of the factors concerning the accurate measurement of various turbulence statistics using hot-wire probes. Results were obtained using a four-wire spanwise vorticity probe in very thick turbulent boundary-layer flows. The scale of the flow field allowed for very good spatial resolution. Descriptions of the flow facility, the experimental conditions and the probe characteristics are given in §§2 and 3. Information concerning the low-speed nature of the present experiments is given in §4. Section 5.1 includes results concerning the measurement of gradients in an anisotropic flow, as well as an evaluation of the effect of the probe's asymmetry on its measurement accuracy. Section 5.2 summarizes results pertaining to the averaging times necessary for adequate statistical convergence as a function of Reynolds number and position in the boundary layer. Section 6 presents further discussion and conclusions.

2. Experimental facilities and conditions

The experiments were performed in the 17 m low-speed wind tunnel in the Turbulence Structure Laboratory at Michigan State University. The test section of this suction tunnel is 17.1 m long, 1.21 m wide and nominally 0.61 m high. The top and one sidewall of the tunnel are made of Plexiglas to allow for flow visualization, and the other two sides are made of plywood. The tunnel is positioned in the centre of a 18.3 m × 30.5 m × 6.1 m pressure and temperature controlled laboratory which acts as the return circuit when the tunnel is used in the closed-return mode. Suction

for the tunnel is provided by a low-noise axial fan, and is kept at constant speed by an eddy current speed controller. The fan assembly is mounted on vibration absorbers and is isolated from the test section via flexible joints. A carefully adjusted set of screens and honeycombs developed via an iterative procedure, and based upon the work of Loerke & Nagib (1977) and deBray (1967), make up the tunnel inlet. This inlet configuration was constructed to avoid the formation of Taylor–Görtler vortices associated with tunnel inlet contractions. The resulting free-stream turbulence intensities at the speeds of the present experiments were less than 0.2%. The tunnel exit consists of a 2:1 axial diffuser followed by a 2:1 radial diffuser. For the present experiments the adjustable top wall of the tunnel was set at a divergence of 0.25° over its entire length, resulting in a differential pressure coefficient, dC_p/dx (where $C_p = dp/\rho U_\infty^2$), of less than ± 0.002; a value well within the tolerance of 0.02 deemed negligible by Murlis, Tsai & Bradshaw (1982). The spanwise uniformity of the flow at the present measurement location is $\pm 2.3\%$ peak-to-peak across the centre 0.46 m as determined by Preston tube surveys (Rashidnia 1985). For more details concerning the flow facility and its qualification the reader is referred to Rashidnia (1985) and Klewicki (1989).

The data acquisition, signal conditioning, and probe positioning apparatus consisted of the vorticity probe (described in §3.1), four DISA 55M01 constant-temperature anemometers, a custom-built analogue signal amplifier, a MKS Baratron model 398 differential pressure transducer, two Krohn Hite model 3323 analogue filters, a Data Translation DT3368/DT3369 simultaneous sample and hold A/D subsystem contained within a PDP 11/23 computer, a cathetometer capable of measuring vertical distances to within 0.01 mm (± 0.001 mm) used to locate the probe centre from the wall, and a vertical traverse mechanism capable of measuring to within 0.0254 mm ($\pm 0.002\,54$ mm).

The zero-pressure-gradient boundary layers studied develop along the lower wall of the flow facility. A 6.35 mm threaded rod was used to trip the flow approximately 0.5 m downstream of the tunnel inlet. Tripping the flow was not necessary to obtain a fully developed state at the measurement station but did serve to localize transition and ensure spanwise uniformity. The measurement station was approximately 15.25 m downstream of the tunnel inlet. A summary of the principal characteristics of the boundary layers at the three Reynolds numbers considered is given in table 1, and logarithmic mean velocity profiles as measured by the spanwise vorticity probe's $\times$-array are presented in figure 1. Determination of the friction velocity was made using the Clauser plot technique, in conjunction with Coles' (1968) law of the wall.

3. The spanwise vorticity probe

3.1. *Physical characteristics*

The spanwise vorticity probe used is similar to that described by Foss, Klewicki & Disimile (1986*b*). However, the calibration and computational scheme used to obtain the vorticity time series is simpler than theirs because boundary-layer flows in general do not generate the large incidence angles encountered in mixing layers and jets. The probe, shown schematically in figure 2, consists of a parallel-array, and a $\times$-array located at the same streamwise (x) position but displaced in the spanwise (z) direction. The spacing of the wires in the parallel array is nominally 1.0 mm, as is the spacing of the slant wires comprising the $\times$-array. The spacing between the centres of the parallel and $\times$-arrays is ≈ 3.4 mm. The slant wires of the $\times$-array are

R_θ	U_∞ (m/s)	δ_{99} (mm)	θ (mm)	H	u_τ (m/s)	C_f	f_c (Hz)	f_s (Hz)
1010	0.607	206	24.8	1.45	0.0282	0.00430	250	500
2870	1.752	205	24.5	1.40	0.0707	0.00325	500	1000
4850	2.981	199	24.3	1.38	0.1125	0.00285	1000	2000

TABLE 1. Principal characteristics of the zero-pressure-gradient boundary layers of the present study; f_c = low-pass cutoff frequency; f_s = sampling frequency

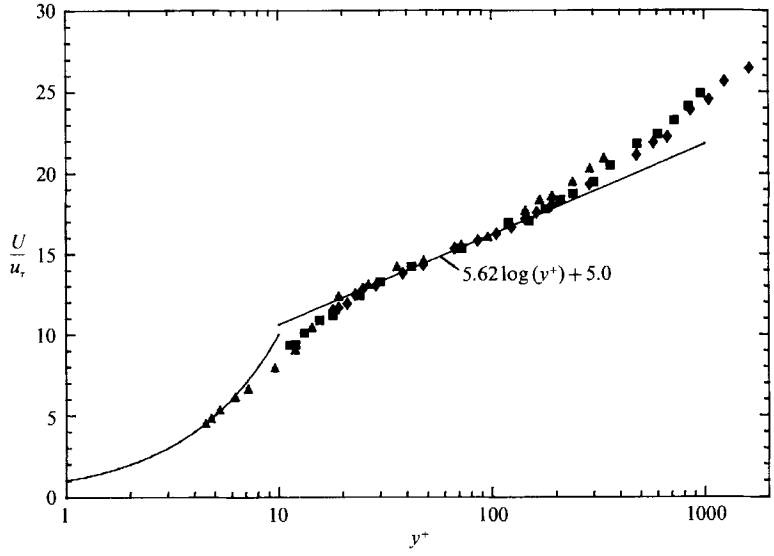

FIGURE 1. Logarithmic mean velocity profiles: ▲, $R_\theta = 1010$; ■, 2870; ◆, 4850.

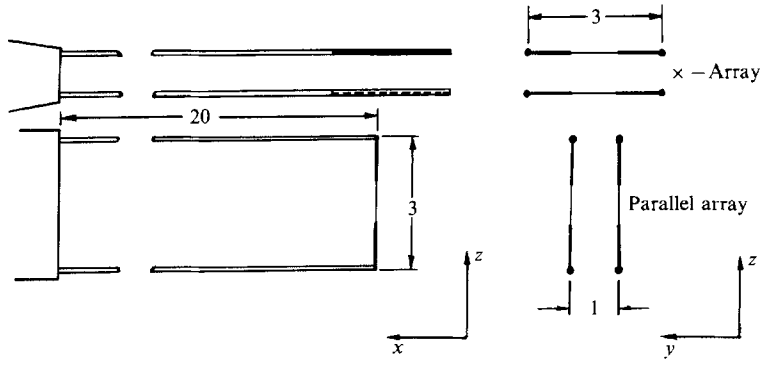

FIGURE 2. Schematic of the spanwise vorticity probe (dimensions in mm).

nominally at an angle of 45° with respect to probe axis; a determination of their 'effective' angles is made during calibration.

The individual tungsten hot-wires are 5 μm in diameter and are copper plated. The copper plating allows the wires to be soft-soldered to the ends of the support prongs, and also aerodynamically isolates the central etched active region from the support prongs. The overall wire length is 3 mm with a centre active region of 1 mm. This

gives a length/diameter ratio of ≈ 200. For the present experiments all of the hot wires were operated at an overheat ratio of 1.7. According to the study of Champagne, Sleicher & Wehrman (1967), under these conditions end heat conduction loss from the wires should be less than 8% of the convective heat loss. The wires of the parallel array are mounted on ≈ 20 mm long jeweller's broaches. The ratio of the broach length to the tapered probe head diameter is about 8. This is believed to greatly reduce possible probe-body effects on the gradient measurements, as discussed by Böttcher & Eckelmann (1985). For further details concerning the probe's physical characteristics, refer to Foss *et al.* (1986*b*).

3.2. *Calibration*

Calibration of the parallel-array wires is performed by fitting the data to an equation of the form $E^2 = A + BV^n$, where the best least-squares fit was chosen from $n = 0.40$ to $n = 0.60$. To minimize errors in $\partial u/\partial y$ due to mismatched calibration of the parallel-array wires, one wire was calibrated with velocities deduced from the pressure transducer and the second wire was then calibrated against the first (a procedure suggested by J. F. Foss, private communication). The calibration procedure used for the $\times$-array is a variation of an 'effective' angle technique (see Signor 1982; Lovett 1982; Klewicki & Falco 1988). All calibrations were performed using mean flow data. Based upon results of Foss, Ali & Haw (1986*a*) no corrections were used to compensate for spanwise velocity contamination of the $\times$-array data. At least one determination of the calibration constants was made both prior to and following each acquisition session.

4. Factors affecting data quality

During the course of this study factors indicative of the experiment quality were thoroughly examined. These factors address issues such as the sampling rate and low-pass cutoff frequencies (see table 1), digitizer resolution, total averaging times (see §5.2), and the methods of data reduction. This information is presented in detail in Klewicki & Falco (1988), and, in general, follows the design criteria of Tennekes & Wyngaard (1972) and/or Antonia, Satyaprakash & Hussain (1982). In the following subsection additional issues concerning uncertainties resulting from the lower flow velocities of this study are discussed.

4.1. *Effects of natural convection from the hot wires*

As a result of the low flow velocities used in the present experiments, questions arose concerning the possible effects of natural convection from the hot wires. For natural convection, the square root of the Grashof number ($Gr \equiv g\beta d^3 \Delta t/\nu^3$) is analogous to the Reynolds number ($R \equiv U_c d/\nu$) of a forced flow, see for example Gebhart (1971). By equating $Gr^{\frac{1}{2}}$ and R, one may deduce a characteristic velocity associated with natural convection to be $U_c = (gd\beta\Delta t)^{\frac{1}{2}}$. Using this relation and the parameters pertinent to the present measurements,

$$d = 5 \times 10^{-6} \text{ m}$$
$$\Delta t = 205 \text{ °C}$$
$$\beta \approx 2.5 \times 10^{-3} \text{ °K}^{-1} \text{ (avg)},$$

one finds $U_c = 0.005$ m/s. The lowest mean velocity measured in the $R_\theta = 1010$ boundary layer was 0.127 m/s. Thus, even in the worst case the estimate of the natural convection velocity was only about 4% of the mean. Of course 4% of the

mean could be significant when considering the fluctuating quantities. However, numerous statistics of fluctuating quantities in the near-wall region that should be sensitive to the directional bias imposed by natural convection (for example, the skewness of u and v, have been examined, Klewicki 1989), and none of these data exhibit features leading us to suspect that natural convection has caused quantifiable errors.

4.2. *Free-stream uncertainty*

Because of the relatively low flow speeds and the long integration times involved in the present experiments, it was felt necessary to quantify the variations in the free-stream velocity. In particular, answers to the following two questions were desired: (1) Within a given data record acquisition time, what is the maximum uncertainty associated with possible variations in U_∞, and (2) was there a quantifiable change either in the wire calibration constants or the free-stream conditions over the duration of an entire measurement session?

4.2.1. *Variations in U_∞ during a single record*

In order to quantify the effects of possible variations in U_∞ it is insufficient to simply measure the variation in the mean velocity over the duration of a data record (say by computing the variance of an ensemble of short-time averages), because changes in the mean velocity do not necessarily provide an accurate measure of this effect on fluctuating quantities. Instead, a better measure would be to examine this effect on the fluctuations directly. One would expect the higher-order odd moments to be most sensitive to mean variations. In general, however, odd moments tend to converge very slowly, and thus the use of the variance of a skewness over a given data record would also include additional convergence error. Given these considerations, it was decided to quantify the possible effects of variations in U_∞ by observing the maximum percent variation in $\langle uv \rangle$ from its final converged value at $y/\delta \approx 0.37$. This variable was chosen since it is both an odd moment (i.e. the first) of a turbulence quantity, and it converged quite rapidly. The criterion was employed at $y/\delta \approx 0.37$ since, in general, statistics in this region converged most rapidly. Thus, a criterion was established that best isolates the convergence errors from those that result from variations in U_∞ during a given data record. The uncertainty as indicated by this criterion for the $R_\theta = 1010$, 2870 and 4850 boundary layers is 1.9, 1.5 and 1.2% respectively. These values were interpreted as the 'noise' level in the analysis of statistical convergence summarized in §5.2.

4.2.2. *Effects of long-term variations in experimental conditions*

A considerable effort was made in ensuring that calibration drift errors were minimized. Essentially, the quality control of calibration drift errors was maintained by comparing the calibrations performed both before and after each experiment. In the event of discernible calibration drift, the experiment was repeated (see Klewicki & Falco 1988).

Since there was good climate control within the laboratory (± 0.25 °C and no detectable variation in pressure), the variation in U_∞ over the duration of an entire experiment could be attributed to the performance of the fan speed controller/motor. To measure this performance, a reproducibility experiment was run that consisted of positioning the ω_z probe at $y^+ \approx 6.2$ in the $R_\theta = 1010$ boundary layer and acquiring five data files at equal time intervals over a period of approximately eight hours. (Note that in all experiments described herein the electronics and flow facility were

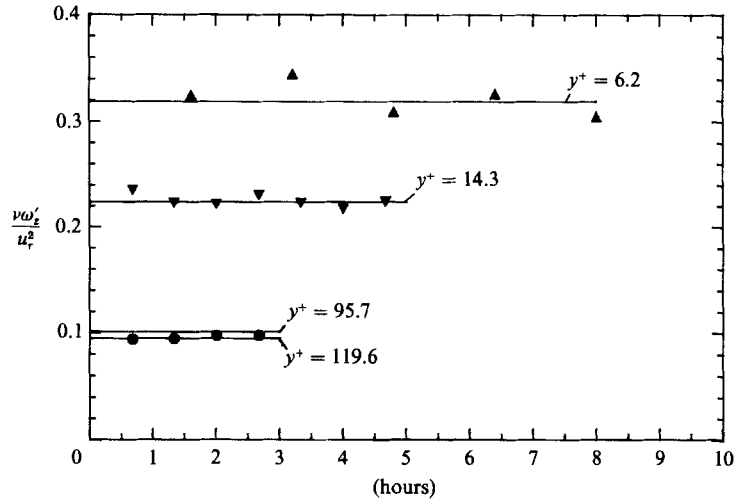

FIGURE 3. Measured $\omega_z'\nu/u_\tau^2$ values at different locations in the $R_\theta = 1010$ boundary layer as a function of experiment time: ▲, auxillary experiment $y^+ \approx 6.2$; ▼, correlation experiment $y^+ \approx 13.4$; ●, correlation experiment $y^+ \approx 100.5$; solid lines represent values from the $R_\theta = 1010$ distribution of figure 11 at the y^+ values indicated.

allowed to 'warm-up' for at least $1\frac{1}{2}$ hours). Furthermore, comparisons are made with results derived from the stationary probe of the two-point ω_z correlation measurements of Klewicki (1989). The length of each data record of the reproducibility experiment was 20% of the record used at $y^+ = 6.2$ in figure 11. The results of this experiment, in terms of $\omega_z'\nu/u_\tau^2$, as well as the data from the correlation experiments (with probes fixed at $y^+ \approx 13.4$ and 100.5) are given as a function of the run time in figure 3. The horizontal lines represent data taken from the distribution of figure 11. A least-squares fit of each of the three data sets in figure 3 was made using the model $\omega_z' = B_0 + B_1 t$ (where t is the run time). Given the assumptions of additive, zero mean, constant variance, uncorrelated, and normally distributed errors associated with the measurement of ω_z' as a function of run time, and that the parameters B_0 and B_1 are non-random, an F test of these results indicate that one cannot reject the hypothesis that $B_1 = 0$, to a level of significance of 0.99. Thus, it was concluded that over extended periods of time U_∞ did remain constant. Note also that the results of the reproducibility experiment show a much greater variation about the data of figure 11 than the results of the correlation experiments – which had much longer averaging times. As a result of the relatively small sample sizes used in the reproducibility experiment, a good part of this point-to-point variation is probably attributable to incomplete convergence. This conclusion is further supported by the results in §5.2.

To obtain an error bar on ω_z', standard deviations were computed from the data of figure 3. The errors bars in figure 11 represent ± 1 standard deviation. The maximum standard deviation (at $y^+ = 6.2$) is 4.6% of the measured value. The agreement between the mean values of the data of figure 3 and the corresponding points in the distribution of figure 11 are within ± 2% (thus indicating an ability to accurately reproduce the free-stream condition). Furthermore, the largest error bar represents a maximum error estimate for all of the distributions (Klewicki & Falco 1988).

As a final comment, it should be noted that no wire breakages occurred over the time necessary to acquire the three R_θ distributions.

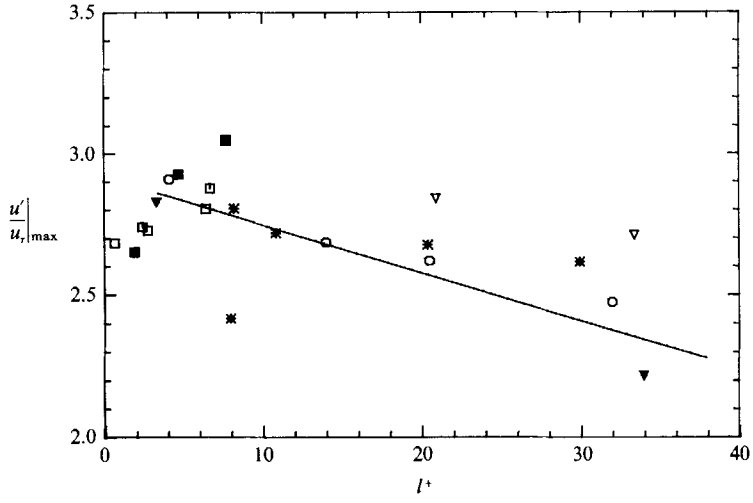

FIGURE 4. The maximum non-dimensional axial intensity as a function of sensor length in viscous units: ■, present data; □, Wei (1987); ⊡, Ueda & Hinze (1975); ✱, Purtell *et al.* (1981); ▽, Andreopoulos *et al.* (1984); ▼, Ligrani & Bradshaw (1987); ○, Johansson & Alfredsson (1983).

5. Results

In this section results pertaining to spatial/temporal resolution and averaging times necessary for statistical convergence are presented, and compared with other wall flow studies. Section 5.1 presents results (along with support from previous studies) which are used to deduce conclusions pertaining to the spatial and temporal resolution needed to accurately resolve near-wall physics using hot-wire probes. Also included in §5.1 is information specifically pertaining to the validity and accuracy of the present measurements. Section 5.2 presents the results concerning averaging times necessary to obtain statistical convergence.

5.1. *Spatial resolution*

Assessing the overall effect of finite spatial resolution on multi-wire probe measurements is difficult because of numerous contributing factors that are involved. In general, however, it appears to be fairly well documented that increasing the spatial scale of a probe will result in an attenuation of the statistical moments of the probe's signal. Given wires with sufficiently large length-to-diameter ratios, this attenuation can be caused by two major effects. Finite-wire-length effects tend to average high-amplitude small-scale fluctuations with spatially adjacent low-amplitude motions over the length of the sensing element. Finite-wire-spacing effects tend to spatially filter derivative signals at wavelengths about equal to the wire spacing. Both of these effects, primarily by causing a failure to resolve high-amplitude fine-scale information represented in the tails of a given probability distribution, will generally cause an attenuation in the measured values of both the even and odd moments of that distribution.

5.1.1. *Wire length effects*

An indicator of wire length effects on wall flow velocity measurements is the maximum measured value of u'/u_τ. Figure 4 presents the maximum value of u'/u_τ versus the non-dimensional wire length as found using the parallel-array wire closest to the wall, and from other wall flow investigations. Also included is a curve fit of the

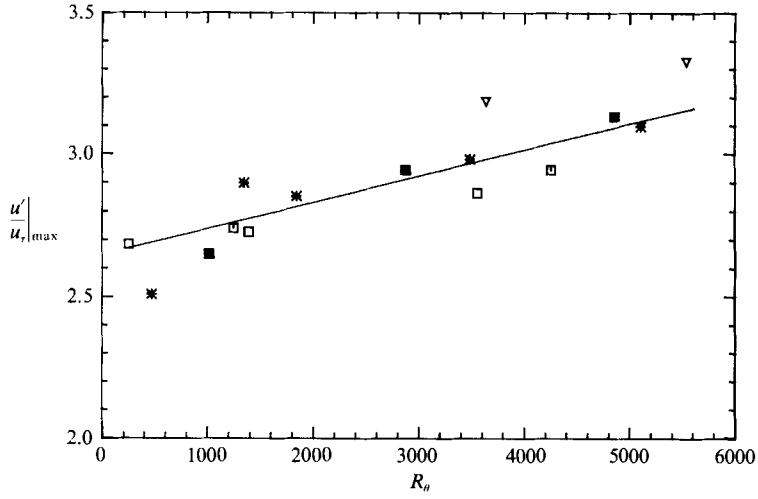

FIGURE 5. The maximum non-dimensional axial intensity as a function of R_θ, symbols same as in figure 4; solid line represents a linear least-squares curve fit given by $(u'/u_\tau)_{\max} = 2.616 + (0.000092)\,R_\theta$.

data of Johansson & Alfredsson (1983) and Ligrani & Bradshaw (1987). This curve fit shows that, at a given Reynolds number, if one increases the length of a sensor the peak value of u'/u_τ will decrease. However, the variation in the peak value of u'/u_τ cannot be explained in terms of non-dimensional wire length alone. For example, the present data, those of Wei (1987), and Ueda & Hinze (1975) (all having $l^+ < 8$) show a consistent decreasing trend as probes of smaller l^+ are used. Furthermore, the data of Purtell, Klebanoff & Buckley (1981) as well as those of Andreopolous *et al.* (1984) apparently contradict the trend shown by the curve fit. In the case of Purtell *et al.*, a difference of 15% in the peak value is obtained for probes of nearly identical $l^+ \approx 8$, and then for larger l^+ the attenuation is less severe than either the Johansson & Alfredsson or Ligrani & Bradshaw data. In the case of Andreopolous *et al.*, their data are roughly 15% higher than those predicted by the curve fit.

To gain an understanding of this apparent scatter, the possibility of a Reynolds-number dependence was examined. To do this, the curve fit of figure 4 was used to correct the data by removing the attenuation caused by finite-probe-scale effects. (Note that the use of this curve fit implies the assumption that the attenuation is only a function of the non-dimensional sensor length scale, l^+.) Figure 5 presents the corrected data of figure 4 as a function of Reynolds number. This figure clearly suggests that the true peak u'/u_τ value is Reynolds-number dependent. Note that only the data of Purtell *et al.* (for wire lengths $l^+ \approx 10.9$, 20.4, 29.9), and those of Andreopolous *et al.* ($l^+ \approx 20.9$, 33.4) actually required the correction for spatial attenuation in order to exhibit this trend. This apparent Reynolds-number dependence explains why the lower Reynolds number data of Purtell *et al.* are 15% lower, and why the data of Andreopolous *et al.* are 15% higher than suggested by the curve fit in figure 4.

Apparently there are, in practice, competing effects between an increase in $u'/u_\tau|_{\max}$ as a result of a Reynolds-number dependence in its true value (over the given R_θ range), and an attenuation in its measured value resultant from finite-probe-scale effects. Given that many lower resolution studies in wall flows indicate that the maximum in u'/u_τ decreases as the Reynolds number is increased, detecting

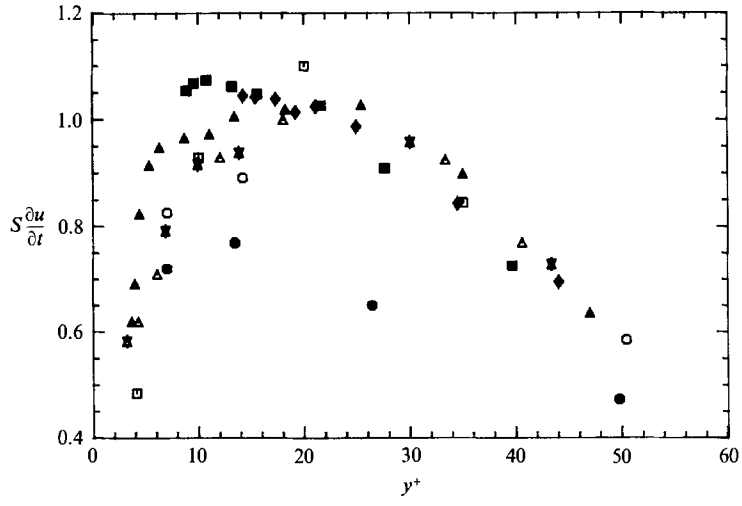

FIGURE 6. Near-wall distributions of the skewness of $\partial u/\partial t$: present data symbols same as in figure 1; ✡, Wallace *et al.* (1977); △, □, Ueda & Hinze (1975); ○, ●, Johansson & Alfredsson (1983); for probe scale information and Reynolds numbers see table 2.

the opposite may provide a simple measure of the minimum probe spatial resolution necessary to study Reynolds-number effects. Assuming the above conclusion, the data of Purtell *et al.* show the correct Reynolds-number dependence for small l^+, but then with increasing Reynolds number (thus, increasing the non-dimensional probe scale) an opposite trend is observed. It therefore appears that the attenuation effect is stronger than the demonstrated Reynolds-number effect for the given R_θ range.

To gain an understanding of the effect of wire length on time-derivative statistics, the values of the skewness of $\partial u/\partial t$ in the near-wall region were examined. The present results, shown in figure 6, are from the same wire used to derive the data in figure 4. Data from other channel and boundary-layer investigations are also shown (see table 2). The generally good agreement between the present data and those of Wallace, Brodkey & Eckelmann (1977) and Ueda & Hinze (1975) for $y^+ \geqslant 15$ probably reflects the fact that the spatial resolution (either wire length and/or wire spacing) of the probes in all of these investigations is about equal. It should be noted that Reynolds-number effects apparently do not significantly manifest themselves in this region of the flow over the range $300 < R_\theta < 5000$ for this statistic. Furthermore, the data of Johansson & Alfredsson show attenuation resultant from using larger probes ($l^+ = 14$, 32). Closer to the wall the data of this figure exhibit considerable scatter (up to 30%) for wire lengths in the range $5 < l^+ < 15$. In the light of the discussion above concerning u'/u_τ this could be caused by spatial resolution and/or Reynolds-number effects. In general, comparison of the high- and low-resolution studies in this figure indicate that wire lengths must be significantly smaller than 14 viscous units.

To further refine when attenuation caused by finite-probe-scale effects becomes significant, estimates of the $S(\partial u/\partial t)$ have been obtained from the ×-array data of the ω_z probe. As the Reynolds number increased these profiles showed an identifiable decrease in the magnitude for $y^+ < 50$. This trend is consistent with the additional spatial averaging effects resulting from the wire spacing of the ×-array. (Note that the u'/u_τ profiles derived from the ×-array follow the R_θ trend exhibited by the curve

Studies(s)	Fig.(s)	Symbol	Reynolds number	Probe type	Probe scale in viscous units
Ueda & Hinze (1975)	4, 5, 6	□ △	$R_\theta = 1244$	Single	2.7
	4, 5, 6	□	$R_\theta = 4248$	wire	6.7
Andreopoulos *et al.* (1984)	4, 5	▽	$R_\theta = 3624$	Single	20.9
	4, 5	▽	$R_\theta = 5535$	wire	33.4
Purtell *et al.* (1981)	4, 5	✱	$R_\theta = 465$	Single	8.0
	4, 5	✱	$R_\theta = 1340$	wire	8.2
	4, 5	✱	$R_\theta = 1840$		10.9
	4, 5	✱	$R_\theta = 3480$		20.4
	4, 5	✱	$R_\theta = 5100$		29.9
Wallace *et al.* (1977)	6	✡	$R_{d/2} = 3850$	×-array	1.9
Johansson & Alfredsson (1983)	4	○	$R_{d/2} = 25000$	Single	4, 14, 21, 32
	6	○ ●	$R_{d/2} = 25000$	wire	14, 32
Ligrani & Bradshaw (1987)	4	▼	$R_\theta = 2620$	Single wire	3.3, 34
Wei (1987)	4, 5	□	$R_{d/2} = 2970$	LDA	0.66
	4, 5	□	$R_{d/2} = 14914$		2.76
	4, 5	□	$R_{d/2} = 39580$		6.43
Balint *et al.* (1987*a*)	12, 13	✡	$R_\theta = 2100$	9-wire probe	9.5

TABLE 2. Summary information concerning other wall-flow investigation data presented. Note that R_θ indicates boundary-layer flow, and $R_{d/2}$ indicates channel flow. See table 3 for information pertaining to the present probe dimensions

fit in figure 5.) Thus, it appears that spatial averaging has a greater effect on skewness of $\partial u/\partial t$ than on u'/u_τ. This result is consistent with the notion that greater spatial resolution is required to obtain derivative information with the same accuracy as the variable itself.

5.1.2. *Wire spacing effects*

According to the study by Wyngaard (1969), in order to resolve fluctuating velocity gradients in an isotropic turbulent flow the wire separation, h, should satisfy the inequality,

$$1.0 < h/\eta \leqslant 3.33, \tag{1}$$

where, $\eta = (\nu^3/\epsilon)^{\frac{1}{4}}$. In the present study ϵ was estimated using four of the twelve terms,

$$\frac{\epsilon}{\nu} = \left\langle \left(\frac{\partial u}{\partial x}\right)^2 + \left(\frac{\partial v}{\partial x}\right)^2 + 3.5\left(\frac{\partial u}{\partial z}\right)^2 + 2.5\left(\frac{\partial u}{\partial y}\right)^2 \right\rangle. \tag{2}$$

This relation was derived by making the following assumptions:

$$\left\langle \left(\frac{\partial w}{\partial y}\right)^2 \right\rangle = \left\langle \left(\frac{\partial u}{\partial y}\right)^2 \right\rangle, \quad \left\langle \left(\frac{\partial v}{\partial z}\right)^2 \right\rangle = \left\langle \left(\frac{\partial u}{\partial z}\right)^2 \right\rangle,$$

$$\left\langle \left(\frac{\partial v}{\partial y}\right)^2 \right\rangle = \frac{1}{2}\left\langle \left(\frac{\partial u}{\partial y}\right)^2 \right\rangle, \quad \left\langle \left(\frac{\partial w}{\partial z}\right)^2 \right\rangle = \frac{1}{2}\left\langle \left(\frac{\partial u}{\partial y}\right)^2 \right\rangle,$$

$$\left\langle \left(\frac{\partial w}{\partial x}\right)^2 \right\rangle = \left\langle \left(\frac{\partial u}{\partial z}\right)^2 \right\rangle,$$

as well as assuming that the sum of the three cross-derivative terms is negligible. These assumptions are similar to those given by Klebanoff (1954).

R_θ	$\eta^+_{\min}$	$\eta^+_{\max}$	$\Delta y/\eta_{\min}$	$\Delta y/\eta_{\max}$	$\Delta z/\eta_{\min}$	$\Delta z/\eta_{\max}$
1010	1.3	3.2	1.5	0.6	5.0	2.0
2870	1.4	5.3	3.4	0.9	11.1	3.0
4850	1.7	7.0	4.6	1.1	15.6	3.8

TABLE 3. Normalized spanwise vorticity probe dimensions; $\eta^+ = \eta u_\tau/\nu$; $\eta_{\min}$ and $\eta_{\max}$ refer to minimum and maximum measured Kolmogorov scales found in each R_θ distribution (η computed from ϵ estimate of equation (2)). The individual wire length and $\times$-array spacing are about equal to Δy

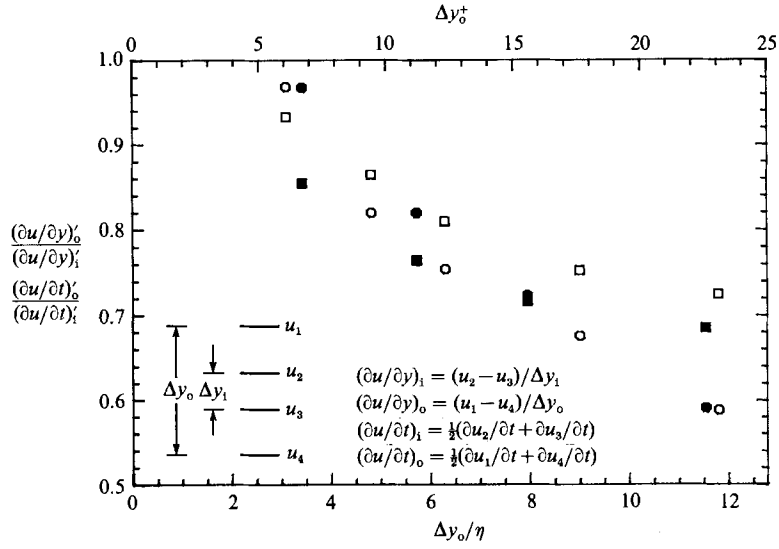

FIGURE 7. Attenuation of gradient intensity ratios as a function of the non-dimensional outer array wire separation (see insert) in the $R_\theta = 1010$ boundary layer: solid symbols, $y^+ \approx 38$; open symbols, $y^+ \approx 53$; ■, □, $(\partial u/\partial t)'_o/(\partial u/\partial t)'_i$; ●, ○, $(\partial u/\partial y)'_o/(\partial u/\partial y)'_i$.

Table 3 presents a summary of the minimum and maximum non-dimensional wire separations encountered in the three boundary layers of the present study. In this table Δy represents the wire spacing in the parallel array, and Δz represents the separation between the centres of the parallel and $\times$-arrays. It should be noted that the resolution of ω_z does not depend on gradients in the spanwise direction. However, the given probe arrangement does assume that $\partial v/\partial x$ at z equals $\partial v/\partial x$ at $z + \Delta z$. Thus, the validity of this assumption, as well as the validity of (1) under anisotropic conditions were examined. Furthermore, since many multi-wire probes use spatial averages of temporal and streamwise derivatives to approximate measurements at the given probe centre, the effect of wire separation on this process was also examined.

An evaluation of wire spacing effects on the measured value of the associated spatial gradient was accomplished by performing an experiment that simultaneously measured $\partial u/\partial y$ fluctuations at the same location using probes that had different wire separations. The experiment's geometry consisted of fixing a parallel array about a given point in the boundary layer, and then positioning a pair of y-traversable single-wire probes at equal Δy spacings above and below the parallel array. The arrangement is shown as an insert in figure 7. In this figure, Δy_i is the wire spacing

between the parallel-array elements, and Δy_0 is the spacing between the two single-wire probes. Simultaneous data from all four wires were taken for various Δy_0, while keeping the centre position of Δy_i and Δy_o the same. The experiment was performed at $y^+ \approx 53$ and at $y^+ \approx 38$ in the $R_\theta = 1010$ boundary layer.

Results pertaining to the attenuation in the measured r.m.s. of $(\partial u/\partial y)_o$ $(\equiv (\partial u/\partial y)'_o)$ as Δy_o was increased are given in figure 7. Data in this figure are presented as the ratio of $(\partial u/\partial y)'_o$ over $(\partial u/\partial y)'_i$. Since data from all four wires were taken simultaneously for each Δy_o, presentation in this way largely eliminates the effect of the observed $\pm 3\%$ variation in $(\partial u/\partial y)'$ from run to run. It is important to note that for the given boundary layer $\Delta y_i^+ \approx 1.84$, and $\Delta y_i/\eta \approx 1.04$ and 0.94 at $y^+ \approx 38$ and 53 respectively. The data in figure 7 are therefore equal to 1.0 at these values and not at the origin. One thing to notice about both the $y^+ \approx 38$ and $y^+ \approx 53$ data is that for $\Delta y/\eta \leqslant 3$ very little attenuation ($\approx 3\%$) occurs, and that changing the level of mean shear appears to have little effect. This suggests that Wyngaard's estimate (equation (1)) is valid to a good approximation, even under anisotropic conditions. Another thing to note is the rapid attenuation ($\sim 15\%$) for wire spacings between $\Delta y/\eta = 3$ and 6.

The present results are seemingly in contrast to those of Böttcher & Eckelmann (1985), which predict that the inner array should give smaller r.m.s. values than the outer array for small Δy_o. To better clarify the source of this discrepancy, Klewicki (1989), using the analysis procedure of Böttcher & Eckelmann, evaluated the performance of the parallel array (contained in the ω_z probe) in measuring the mean gradient, $\partial U/\partial y$. The study revealed that the observed attenuation in the measured mean gradient was generally much smaller than predicted by the Böttcher & Eckelmann study. Furthermore, the observed trends with increasing probe Reynolds number suggested the presence of a constant additive error source rather than an error source proportional to the mean gradient – as predicted by Böttcher & Eckelmann. It is at present believed that the most significant factor responsible for the difference between the present results and those of Böttcher & Eckelmann concerns the probe construction; specifically relating to how well the individual elements of the parallel array are isolated from the flow disturbance effects of the probe body, prongs and the other element (see §3.1).

In order to quantify spatial filtering effects of finite wire separation, spectra Φ of the individual $(\partial u/\partial y)_i$ and $(\partial u/\partial y)_o$ time series were computed. Examples of the frequency spectra for $\Delta y/\eta = 0.94$, 4.83 and 9.01 at $y^+ \approx 53$ are presented in figure 8. By using the wire spacing to construct an approximate frequency, $f_{\Delta y} = U_1/(2\pi\,\Delta y)$, it is clear that the effect of wire spacing is to attenuate the gradient intensity at higher frequencies. Furthermore, creating separate spectral plots from each pair of simultaneously acquired $(\partial u/\partial y)_i$ and $(\partial u/\partial y)_o$ time records allowed for the determination of approximate effective low-pass cutoff frequencies (the frequencies at which the $(\partial u/\partial y)_o$ spectra diverged from the $(\partial u/\partial y)_i$ spectra). These results, as derived from the $y^+ \approx 53$ data, are presented in figure 9 as a function of outer wire separation. In this figure the ordinate is the ratio of the approximate cutoff frequency over f_K, where $f_K \equiv U_1/(2\pi\eta)$. The error bar in figure 8 represents the data scatter at 1 Hz, and was used in discerning the cutoff frequencies in figure 9.

Interesting results concerning how noise in the velocity signals enters into the $\partial u/\partial y$ signals are also described in figure 8. For the present data it is expected that at the highest measured frequencies the energy in the u-spectra is attributable entirely to electronic noise. This noise level, labelled ϵ_u^2 in figure 8, is associated with the white-noise portion of the spectrum at high frequencies. For the u-spectra in this

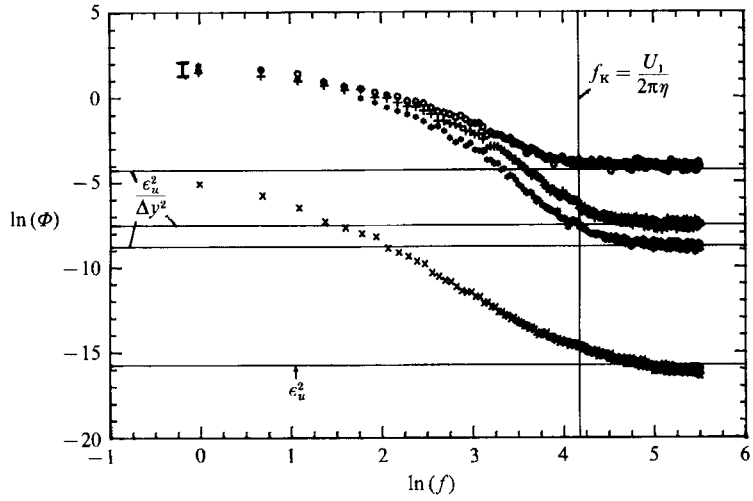

FIGURE 8. Frequency spectra of $\partial u/\partial y$ at $y^+ \approx 53$ in the $R_\theta = 1010$ boundary layer for different Δy spacings: ○, $\Delta y/\eta = 0.94$; +, $\Delta y/\eta = 4.83$; ✱, $\Delta y/\eta = 9.01$. The horizontal lines through the $\partial u/\partial y$ spectra are the electronic noise levels as predicted by $\Phi(\partial u/\partial y) = \epsilon_u^2/\Delta y^2$; where ϵ_u^2 is the energy level of the electric noise in $\Phi(u)$.

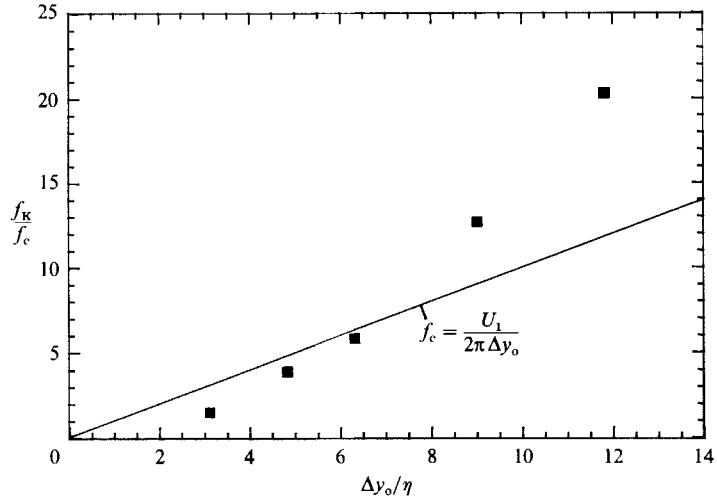

FIGURE 9. Approximate cutoff frequencies of $\Phi(\partial u/\partial y)$ due to the spatial filtering effect of finite wire separation (point of divergence with the $\Delta y/\eta = 0.94$ curve) as a function of non-dimensional wire spacing.

figure (derived from the lower wire of the inner array) ϵ_u^2 is about $e^{-15.75}$ ft^2/s or, equivalently, less than 0.3 mV. By assuming that the ϵ_u^2 from the wires are uncorrelated, in the noise-dominated part of the spectrum one may then approximate $\Phi(\partial u/\partial y)$ by $\epsilon_u^2/\Delta y^2$. Using this relation and the above-cited value for ϵ_u^2 allowed estimates of the associated noise levels in $\Phi(\partial u/\partial y)$ for the various Δy to be made. The predicted noise levels are indicated by the horizontal lines. As can be seen, the predicted values agree very well with the actual noise levels in the $\partial u/\partial y$-spectra. These results suggest that the noise level in a single velocity signal can be used to determine the minimum acceptable Δy spacing used to measure $\partial u/\partial y$.

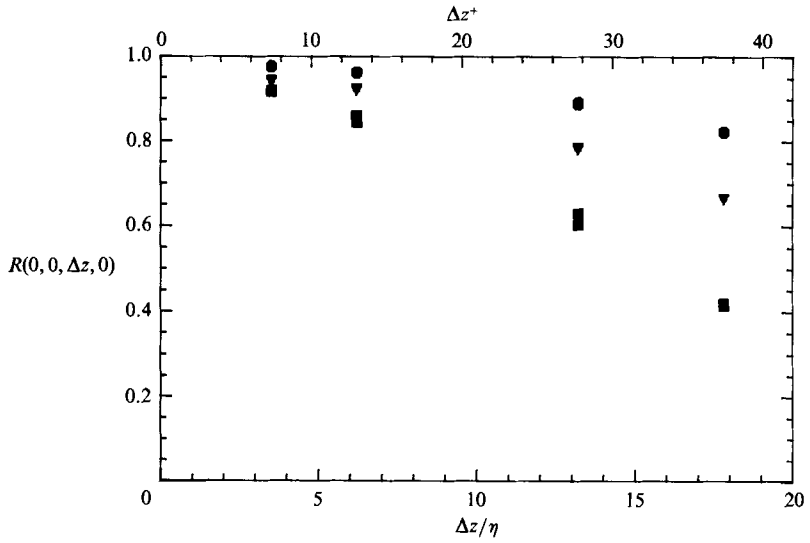

FIGURE 10. Correlation coefficients of u, v and $\partial v/\partial x$ as a function of spanwise separation, Δz, at $y^+ \approx 140$ in the $R_\theta = 1010$ boundary layer: ●, $R_u(0,0,\Delta z,0)$; ▼, $R_v(0,0,\Delta z,0)$; ■, $R_{\partial v/\partial x}(0,0,\Delta z,0)$.

Another problem associated with multi-wire array measurements is the need to average the same quantity obtained at two spatial locations in order to approximate point-wise measurements at the probe centre. The data of the above-described experiment provided a means to assess possible effects of this averaging procedure. For each wire a $\partial u/\partial t$ time series was computed. Then at each instant a spatial average of $\partial u/\partial t$ was computed using the inner two wires and the outer two wires respectively. From these $(\partial u/\partial t)_i$ and $(\partial u/\partial t)_o$ time series, r.m.s. values were computed. As with the $\partial u/\partial y$ data, ratios of r.m.s. $(\partial u/\partial t)_o\,(\equiv(\partial u/\partial t)'_o)$ over $(\partial u/\partial t)'_i$ are presented in figure 7. The most significant attenuation shown in these results is for wire spacings $\Delta y/\eta \leqslant 15$. This attenuation continues, only more slowly, for greater Δy_o values. Clearly, for a given non-dimensional wire spacing, the effect of increasing the mean shear (i.e. moving closer to the wall) is to promote further attenuation in this averaging procedure. Note that this effect is not apparent in the $\partial u/\partial y$ data. It is also interesting to note that the attenuation of $(\partial u/\partial t)'$ for small Δy is greater than that of $(\partial u/\partial y)'$. These results suggest that significant changes in the temporal gradients exist across Kolmogorov-scale eddies. This spatial sensitivity in the temporal gradients was also suggested in the discussion of figure 6.

It should be noted that the utility of the results in figures 7–9 depends on the absolute accuracy of the inner-array results. Of course, the absolute values of $(\partial u/\partial y)'$ are not easily verifiable. However, for the $\partial u/\partial t$ data no statistically significant difference was found between $(\partial u/\partial t)'_i\,(\Delta y/\eta \approx 1)$, and $(\partial u/\partial t)'$ derived from the individual wires of the inner array.

An assessment of the validity of the assumption:

$$\frac{\partial v}{\partial x}\text{ at }(z) \quad = \quad \frac{\partial v}{\partial x}\text{ at }(z+\Delta z)$$

(required to compute ω_z from the present probe) was made by spatially separating two ×-arrays in the spanwise direction and computing the $\partial v/\partial x$ correlation coefficient for various Δz separations. The results of this test are shown in figure 10

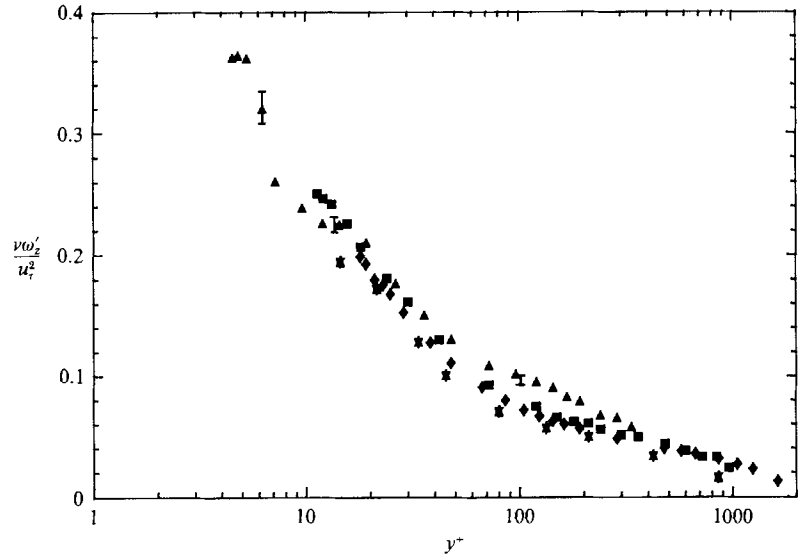

FIGURE 11. Inner variable non-dimensionalization of the r.m.s. spanwise vorticity distribution: present data symbols same as in figure 1; ✡, Balint *et al.* (1987*a*). Error bars at $y^+ = 6.2$, 13.4 and 100.5 are derived from the data of figure 3.

as a function of the non-dimensional spanwise spacing at $y^+ \approx 140$ in the $R_\theta = 1010$ boundary layer. Two runs were made per Δz spacing to increase confidence in the results. Also included in this figure (for reference) are the u- and v-correlation coefficients.

These results show, for example, that at $y^+ = 140$ an average error of approximately 20% can be expected in the instantaneous $\partial v/\partial x$ values for Δz separations of approximately 7η (which is ≈ 19 viscous scales at the given position in the boundary layer). Examination of table 2 shows that in the $R_\theta \approx 1010$ boundary layer the separation between the parallel and the $\times$-array centre is always less than $\eta = 7$. Most of the $R_\theta = 2870$ data, and about half of the $R_\theta = 4850$ data satisfy this condition. However, these results should be viewed with some reservation since, in general, integral scales decrease as the wall is approached, and a significant Reynolds-number dependence may exist for this correlation coefficient. In any case, these results suggest that $\partial v/\partial x$ (and probably all v-gradients) are largely comprised of small-scale contributions, and thus attempts to resolve v-gradients over wire spacings much greater than a few Kolmogorov scales will result in significant errors. Foss *et al.* (1986*a*) support these findings with results from a similar experiment done in a free-shear flow. On the plus side, however, the contribution of this error to spanwise vorticity statistics is diminished in the near-wall region since in this region $(\partial u/\partial y)'$ dominates $(\partial v/\partial x)'$.

5.1.3. *The resolution of* ω_z

To investigate probe-scale effects on ω_z' the distributions of two different non-dimensional functions containing ω_z' were examined.

Figure 11 shows an inner-variable normalization versus y^+. As can be seen, this normalization apparently scales the data. This conclusion is reinforced by the fact that at a given y^+, ω_z' for the present data varies by a factor of greater than ten. An explanation of the error bars presented in this figure was given in §4.2.

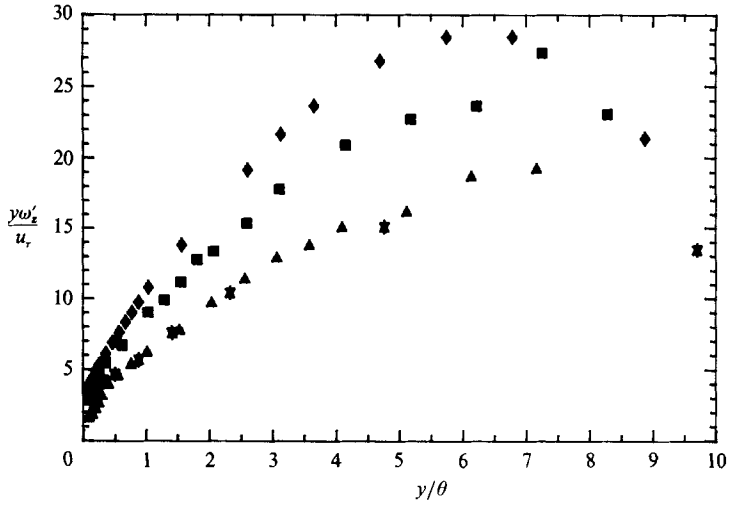

FIGURE 12. The r.m.s. spanwise vorticity normalized by the function y/u_τ and plotted versus y/θ. Symbols same as in figure 11.

The results of this figure also suggest that spatial-resolution effects attenuate both the present data and the data of Balint *et al.* (1987*a*). In the wall region, a small but identifiable attenuation with increasing R_θ can be observed. This attenuation (for the present data) is consistent with a decrease in spatial resolution resulting from an increased non-dimensional probe scale caused by an increase in the Reynolds number. More specifically, given that $(\partial u/\partial y)'$ dominates $(\partial v/\partial x)'$ in the inner region, the observed attenuation probably represents the increase in the Δy^+ between the parallel-array wires as R_θ increases.

To further examine the spatial resolution effects suggested in figure 11, an alternative non-dimensional function containing ω_z' was examined. Figure 12 shows distributions of $y\omega_z'/u_\tau$ *vs.* y/θ. Representing the data in this manner shows a distinct Reynolds-number trend in the opposite direction to that predicted by spatial-resolution effects. Given this Reynolds-number dependence (and assuming that at each R_θ this function is represented by a single curve), the distribution of Balint *et al.* ($R_\theta = 2100, h^+ \approx 8.9$) should lie between the two lower Reynolds-number distributions of the present study. The fact that it does not is probably because of their larger h^+. This figure indicates that their measurements show an attenuation between 10 and 15%. This result is in remarkable agreement with the findings in figure 7.

5.2. *Convergence of turbulence statistics*

Typically, studies examining the convergence of turbulence statistics pay little attention to global effects such as the level of mean shear and the overall Reynolds number. Wall-bounded shear flows present perhaps the most demanding conditions for obtaining acceptable statistical convergence. Intermittently fluctuating phenomena are typically difficult to characterize statistically. In boundary layers one has both the turbulent/non-turbulent interface at the outer edge, and the highly intermittent bursting phenomena near the wall.

This section summarizes results of a fairly comprehensive study of factors affecting statistical convergence for a variety of variables in four regions of the boundary layer

(in which the physics are different), over the R_θ range given in table 1. The details of this study may be found in Klewicki & Falco (1988). A short review of analytical/empirical relations concerning the estimation of convergence times necessary to ensure a given accuracy is given by Antonia *et al.* (1982), and thus will not be repeated here. Rather, the goal of this section is both to document some of the factors influencing statistical convergence, and to provide purely empirical guidelines by which to design experiments.

5.2.1. *Methodology*

Cumulative estimates of statistics up to the fourth moment were computed for u, v, uv, $\partial u/\partial t$, $\partial v/\partial x$, $\partial u/\partial y$, ω_z and $v\omega_z$. These estimates were output at regular intervals of 200000 points (the corresponding integration times depend on the sampling rate). The relatively long times between the intermediate averages were chosen to facilitate statistically meaningful convergence results. The convergence data for the above variables were compiled for the three Reynolds numbers given in table 1, and within four zones of the boundary layer ($12 \leqslant y^+ \leqslant 18$, $40 \leqslant y^+ \leqslant 50$, $0.36 \leqslant y/\delta \leqslant 0.40$, $0.75 \leqslant y/\delta \leqslant 0.80$). These zones are identified as 'near wall', 'strong shear', 'weak shear' and 'intermittent' respectively.

Convergence data were compiled so that for each variable the possible effects of Reynolds number and position in the boundary layer could be identified. Statistical convergence was measured in terms of an absolute percent convergence from a final value resultant from using an entire data record. Thus, the data analysis assumed that the final value was the true value. This assumption proved to be valid in the vast majority of cases. The results were compiled in terms of non-dimensional time units, TU_∞/δ, where T is the averaging time. These units were chosen to represent approximate non-dimensional integral timescales.

The variables were divided into three groups: velocities and Reynolds stress, velocity gradients and vorticity, and a velocity–vorticity product. Comparison of averaging times necessary to obtain a given convergence uncertainty were made between variables within a given group, and between the different groups. Furthermore, trends with Reynolds number and zone were identified. The major results of these comparisons are summarized below.

5.2.2. *Summary of convergence results*

Distinct boundary-layer zonal and Reynolds-number trends in convergence were observed for the statistical moments of the u-, v- and uv-fluctuations. These trends showed that increasing either R_θ or decreasing the distance from the wall generally increased the time to convergence. Both of these trends may possibly be lumped into one, which simply states that for these variables increasing the absolute level of mean shear increases the time to convergence. Also, comparisons between the velocities and Reynolds stress showed that the uv-statistics converged at least as fast as either of the measured velocity components.

The convergence of the velocity-gradient statistics showed much smaller zonal and/or R_θ variations than those of the velocity and Reynolds stress statistics. Their convergence did, however, appear to be adversely affected in the intermittent regions both very near and very far from the wall. In terms of absolute time to convergence, the gradient quantities appeared to converge slightly faster than the velocities or Reynolds stress. However, since δ/U_∞ is probably an integral timescale most appropriate for the velocities, the time necessary for convergence normalized by a characteristic time appropriate to the gradient quantities is probably greater than

	Average to ensure ±3% accuracy	R.m.s. to ensure ±3% accuracy	Skewness to ensure ±5% accuracy	Kurtosis to ensure ±5% accuracy
u, v, uv	$1000U_\infty/\delta$	$1000U_\infty/\delta$	$4000U_\infty/\delta$	$2500U_\infty/\delta$
$\partial u/\partial t$, $\partial v/\partial x$, ω_z, $\partial u/\partial y$,	—	$1000U_\infty/\delta$	$3500U_\infty/\delta$	$2000U_\infty/\delta$
$v\omega_z$	$3000U_\infty/\delta$	$1000U_\infty/\delta$	$6000U_\infty/\delta$	$5000U_\infty/\delta$

TABLE 4. Non-dimensional averaging time criteria to ensure the convergence of statistics up to 4th-order moments in boundary-layer flows over the Reynolds-number range $1010 \leqslant R_\theta \leqslant 4850$

TU_∞/δ. The results also suggested that spatial gradients converge considerably more slowly than temporal gradients. These results may be associated with differences between the fine-scale spatial and temporal structure. Also the results indicated that matching experiments by matching R_λ (the microscale Reynolds number $\equiv u'\lambda/\nu$) is not necessarily sufficient to ensure objective comparisons.

The statistics of the velocity vorticity product, $v\omega_z$, required long averaging times to converge relative to the other variables examined. The convergence of $v\omega_z$ statistics is adversely affected by both increasing the level of mean shear and/or the Reynolds number.

Table 4 presents a compilation of general convergence criteria. Note that these criteria are based upon the assumption that one wishes to obtain profiles across the entire boundary layer, and thus, for example, are conservative for data analysis in the weak-shear zone. The criteria in this table indicate the necessity for considerably longer averaging times than was initially expected. It is at present felt that there are three plausible explanations for this. The first is that this subject has never been, to our knowledge, thoroughly investigated in boundary layers, and thus our expectations gained mainly from free-shear flows did not apply. The second is that because of the very good resolution of the probe, more of the high-intensity fine scale-information in the tails of the respective probability distributions, was represented than in earlier studies. And third, the statistical convergence may be profoundly adversely affected by even small levels of 'noise' (as described in §4.2) caused by variations in the free-stream velocity.

6. Discussion and conclusions

This study has examined aspects of hot-wire measurements that are sensitive to the small-scale structure in boundary layers. They may be grouped into two (not necessarily independent) categories relating to the probe's spatial and temporal resolution, and the statistical detail desired.

Based upon the data of figure 5 it appears that the maximum value of u'/u_τ increases with increasing R_θ. Imperfect spatial resolution can hide this dependence because the attenuation (due to increasing wire length in viscous units as a consequence of increasing R_θ) is apparently greater than the increase due to Reynolds number. Thus, detecting this Reynolds-number trend provides an indicator of good probe resolution, and constitutes a criterion for studies investigating Reynolds-number dependence (over the given R_θ range). It is probably true that as a wire of given length becomes greater than about $8u_\tau/\nu$ (as R_θ is increased), attenuation

caused by spatial averaging effects will begin to conceal this trend. The competing effects between spatial resolution and Reynolds number have apparently hidden the true flow physics, and have led many to the belief that the maximum value of u'/u_τ is indeed a constant. In fact, if one were to ignore both of these effects then the data of figure 4 would appear to support this result in that most of these data are located in a narrow band about $u'/u_\tau \approx 2.8$. Furthermore, with regard to previous studies investigating wire-length effects, the present results suggest that Reynolds-number effects are smaller but not small compared to spatial-averaging effects. This result is contrary to the conclusion of Johansson & Alfredsson (1983). Furthermore, the criterion of Ligrani & Bradshaw (1987) is not universal since identifiable attenuation can clearly be seen in figure 4, for $5 < l^+ < 20$. In the discussion of figure 6 results were deduced supporting the notion that the spatial resolution required to obtain accurate velocity-derivative fluctuations is greater than that required for the velocity fluctuations.

The main result concerning wire-spacing effects on the computed value of spatial velocity gradients is that Wyngaard's (1969) criterion (equation (1)) is to a very good approximation valid even under anisotropic conditions. Furthermore, changing the level of mean shear seems to have little effect on the validity of this criterion.

Conversely however, the $\partial u/\partial t$ results indicate that spatially averaging velocity gradients at each instant (say, to approximate pointwise measurements at a probe centre) results in significant attenuation in the subsequent r.m.s. Results of this averaging are also sensitive to the level of mean shear. These results suggest that even for probes with small off-centre sensing elements (say greater than 3η) one is probably better off accepting non-centred measurements rather than computing an instantaneous spatial average. For example, for the present probe geometry one would probably not improve the accuracy of the estimated value of $\partial v/\partial x$ at the probe centre by adding another $\times$-array at $-\Delta z$ from the parallel-array centre, and then instantaneously averaging over the $2\Delta z$ separation between the two $\times$-arrays.

These results also suggest that there are differences between the temporal and spatial structure of the fine-scale motions in the wall region. Further experiments on these differences (especially as a function of Reynolds number) may lead to new insights concerning the conflicting results (at very different Reynolds numbers) of Willmarth & Bogar (1977) and Johnson & Eckelmann (1983) as discussed in §1.

The results in figure 8 give a good indication of how electronic noise in the velocity signals enters into the $\partial u/\partial y$ signals. It was demonstrated that to a very good approximation $\Phi(\partial u/\partial y) \approx \epsilon_u^2/\Delta y^2$ in the noise-dominated part of the spectrum. This relation allows one to optimize the choice of Δy for a given system noise level by simply performing a single-wire measurement. The data of figure 8 was also used to demonstrate that the main effect of finite wire separation is to remove energy from frequencies higher than an approximate cutoff value f_c, defined as $U_1(2\pi\Delta y)$.

The assumption that the instantaneous values of $\partial v/\partial x$ at (z) equals $\partial v/\partial x$ at $(z+\Delta z)$, specific to the current ω_z probe, proved to have an average accuracy of about 80% for $\Delta z/\eta \approx 7$ in the logarithmic region of the $R_\theta = 1010$ boundary layer. Thus, for the present study its validity is primarily in question for the inner part of the highest R_θ distribution.

Concerning the experiment quality, it was documented that uncertainties associated with the low speeds of the present experiments were small. Also, the matching calibration procedure used for the parallel-array elements proved to eliminate detectable correlated errors in $(\partial u/\partial y)'$. Figure 8 shows this indirectly in that virtually all of the noise in $\Phi(\partial u/\partial y)$ may be attributed to electronic noise.

The statistical convergence study led to the conclusion that as a result of sensitivity to the level of mean shear, the intermittency level, and Reynolds-number effects, existing convergence formulae should be used with caution in wall flows. Also, one should not apply criteria developed in other flow fields to wall-flow studies. For example, at the centreline of a turbulent jet (with a centreline velocity equal to U_c and a transverse scale of L_0) Antonia *et al.* (1982) show that it takes a time of approximately $12L_0/U_c$ to obtain $\pm 5\%$ accuracy in the skewness of $(\partial u/\partial t)$. This criterion, applied to boundary-layer flows (using δ and U_∞) is orders of magnitude smaller than that cited in the present study or in the study of Mestayer (1982).

This work was supported under AFOSR contract 87-0047. The contract monitor was Dr J. McMichael. Also J.C.K. would like to acknowledge the help of Professor J. F. Foss, C. P. Gendrich, and S. J. Ali.

REFERENCES

ALFREDSSON, P. H., JOHANSSON, A. V., HARITONIDIS, J. H. & ECKELMANN, H. 1988 *Phys. Fluids* **31**, 1026.

ANDREOPOULOS, J., DURST, F., ZARIĆ, Z. & JOVANOVIC, J. 1984 *Exps. Fluids* **2**, 7.

ANTONIA, R. A., BROWNE, L. W. B. & CHAMBERS, A. J. 1985 *Phys. Fluids* **28**, 420.

ANTONIA, R. A., SATYAPRAKASH, B. R. & HUSSAIN, A. K. M. F. 1982 *J. Fluid Mech.* **119**, 55.

BALINT, J. L., VUKOSLAVČEVIĆ, P. & WALLACE, J. M. 1987*a* In *Advances in Turbulence, Proc. First European Turbulence Conf., Lyon, France* (ed. G. Comte-Bellot & J. Mathieu), p. 456. Springer.

BALINT, J. L., VUKOSLAVČEVIĆ, P. & WALLACE, J. M. 1987*b* *Bull. Am. Phys. Soc.* **32**, 2051.

BLACKWELDER, R. F. & ECKELMANN, H. 1979 *J. Fluid Mech.* **94**, 577.

BLACKWELDER, R. F. & HARITONIDIS, J. H. 1983 *J. Fluid Mech.* **132**, 87.

BLACKWELDER, R. F. & KOVASZNAY, L. S. G. 1970 *Rep.* DA-31-124-ARO-D-313. The Johns Hopkins University Dept. of Mech., Baltimore, Maryland.

BÖTTCHER, J. & ECKELMANN, H. 1985 *Exps. Fluids* **3**, 87.

BROWNE, L. W. B., ANTONIA, R. A. & SHAH, D. A. 1987 *J. Fluid Mech.* **179**, 307.

CHAMPAGNE, F. H., SLEICHER, C. A. & WEHRMANN, O. H. 1967 *J. Fluid Mech.* **28**, 153.

COLES, D. E. 1968 In *Proc. of Computation of Turbulent Boundary Layers, AFOSR-IFP-Stanford Conf.* (ed. D. Coles & X. Hirst). Stanford University, California.

CORRSIN, S. & KISTLER, A. L. 1954 *NACA TN* 3133.

DEBRAY, B. G. 1967 *Brit. Aero. Res. Counc. Rep.* 29-271.

ECKELMANN, H., NYCHAS, S. G., BRODKEY, R. S. & WALLACE, J. M. 1977 *Phys. Fluids Suppl.* **20**, S225.

EMMERLING, R. 1973 Bericht Max-Planck-Institut für Stromungsforschung, 9/1973.

FALCO, R. E. 1980 *AIAA*-80-1356.

FOSS, J. F., ALI, S. K. & HAW, R. C. 1986*a* In *Advances in Turbulence, Proc. First European Turbulence Conf., Lyon, France* (ed. G. Comte-Bellot & J. Mathieu), p. 446. Springer.

FOSS, J. F., KLEWICKI, C. L. & DISIMILE, P. J. 1986*b* *NASA CR* 178098.

GEBHART, B. 1971 *Heat Transfer*, 2nd edn, p. 326. McGraw-Hill.

HOGENES, J. G. A. & HANRATTY, T. J. 1982 *J. Fluid Mech.* **124**, 363.

JOHANSSON, A. V. & ALFREDSSON, P. H. 1983 *J. Fluid Mech.* **137**, 409.

JOHNSON, F. D. & ECKELMANN, H. 1983 *Phys. Fluids* **26**, 2408.

KASTRINAKIS, E. G. 1977 Bericht Max-Planck-Institut für Stromungsforschung, 5/1977.

KASTRINAKIS, E. G. & ECKELMANN, H. 1983 *J. Fluid Mech.* **137**, 165.

KASTRINAKIS, E. G., ECKELMANN, H. & WILLMARTH, W. W. 1979 *Rev. Sci. Instrum.* **50**, 759.

KLEBANOFF, P. S. 1954 *NACA TN* 3178.

KLEWICKI, J. C. 1989 On the interactions between the inner and outer region motions in turbulent boundary layers. Ph.D. dissertation, Michigan State University, East Lansing, Michigan.

KLEWICKI, J. C. & FALCO, R. E. 1988 *Rep.* TSL-88-4. Dept. Mech. Eng., Michigan State University, East Lansing, Michigan.

KLINE, S. J., REYNOLDS, W. C., SCHRAUB, F. A. & RUNSTADLER, P. W. 1967 *J. Fluid Mech.* **30**, 165.

KOVASZNAY, L. S. G. 1950 *Q. Prog. Rep. Aero Dept Contract NORD*-8036-JHB-3D. The Johns Hopkins University.

KOVASZNAY, L. S. G., KIBENS, V. & BLACKWELDER, R. F. 1970 *J. Fluid Mech.* **41**, 283.

KOVASZNAY, L. S. G., KOMODA, H. & VASUDEVA, B. R. 1962 In *Proc. Heat Transfer and Fluid Mech. Inst.*, p. 1. Stanford University Press.

KREPLIN, H. P. & ECKELMANN, H. 1979 *Phys. Fluids* **22**, 1233.

LIGRANI, P. M. & BRADSHAW, P. 1987 *Exps. Fluids* **5**, 407.

LOERKE, R. I. & NAGIB, H. M. 1977 *AGARD Rep.* R-598, AD-749-891.

LOVETT, J. A. 1982 The flow fields responsible for the generation of turbulence near the wall in turbulent shear flows. M.S. thesis. Michigan State University.

MESTAYER, P. 1982 *J. Fluid Mech.* **124**, 475.

MURLIS, J., TSAI, H. M. & BRADSHAW, P. 1982 *J. Fluid Mech.* **122**, 13.

PURTELL, L. P., KLEBANOFF, P. S. & BUCKLEY, F. T. 1981 *Phys. Fluids* **24**, 802.

RASHIDNIA, N. 1985 Changes in the turbulent boundary layer structure associated with net drag reduction by outer layer manipulators. Ph.D. dissertation, Michigan State University, East Lansing, Michigan.

ROBERTS, J. B. 1973 *Aeronaut. J.* **77**, 406.

SCHEWE, G. 1983 *J. Fluid Mech.* **134**, 311.

SIGNOR, D. B. 1982 A study of intermediate scale coherent motions in the outer region of turbulent boundary layers. M.S. thesis, Michigan State University.

SUBRAMANIAN, C. S., KANDOLA, B. S. & BRADSHAW, P. 1985 *IC Aero Rep.* 85-01.

TENNEKES, H. & WYNGAARD, J. C. 1972 *J. Fluid Mech.* **55**, 93.

UBEROI, M. S. & KOVASZNAY, L. S. G. 1953 *Q. Appl. Maths* **X**, 375.

UEDA, H. & HINZE, J. O. 1975 *J. Fluid Mech.* **67**, 125.

WALLACE, J. M., BRODKEY, R. S. & ECKELMANN, H. 1977 *J. Fluid Mech.* **83**, 673.

WEI, T. 1987 Reynolds number effects on the small scale structure of a turbulent channel flow. Ph.D. dissertation, University of Michigan, Ann Arbor, Michigan.

WILLMARTH, W. W. & BOGAR, T. J. 1977 *Phys. Fluids Suppl.* **20**, S9.

WILLMARTH, W. W. & SHARMA, L. K. 1984 *J. Fluid Mech.* **142**, 121.

WYNGAARD, J. C. 1968 *J. Phys.* E: *Sci. Instrum.* **1**, 1105.

WYNGAARD, J. C. 1969 *J. Phys.* E: *Sci. Instrum.* **2**, 983.